Fayad *et al. J. Wirel. Commun. Netw.* *(2026) 2026:50*
https://doi.org/10.1186/s13638-026-02592-y

Journal on Wireless Communications and Networking

RESEARCH **Open Access**

Green 6 G: energy-efficient user association and power allocation with locally harvested renewable energy

Abdulhalim Fayad[1,2*], Tibor Cinkler[1,2†], Jeroen Famaey[3†] and István Gódor[4†]

†Tibor Cinkler, Jeroen Famaey and István Gódor have contributed equally to this work.

*Correspondence: fayad@tmit.bme.hu

[1] Department of TMIT, BME, Budapest, Hungary
[2] HUN-REN-BME Cloud Applications Research Group, Budapest, Hungary
[3] IDLab, University of Antwerp – imec, Antwerp, Belgium
[4] Ericsson Research, Budapest, Hungary

Abstract

The rising energy demand in urban 6 G ultra-dense mmWave mobile networks will present economic and environmental concerns. Addressing these issues calls for efficient energy management frameworks that enhance the reliance of 6 G networks on renewable energy sources while minimizing dependence on grid-based power. This is particularly important as base stations (BSs) are the most energy-intensive components in these networks. This paper focuses on the problem of *User Association with Green Power Maximization*. We propose intelligent load-based on–off switching mechanisms for grid-powered microbase stations (μBSs) and integrate renewable energy through energy harvesting techniques. The aim is to reduce the grid-power consumption and promote sustainable 6 G network operations. We formulate the problem as an integer linear pGUASrogram to find the optimal solution. Moreover, we propose three heuristic solutions: greedy green user allocation strategy, random user allocation strategy, and sequential user allocation strategy. We considered two dynamic μBS power models: a stepwise and a load-based linear model. We evaluated our proposed solutions via simulations with both power models. Finally, we provide insights into how these solutions can significantly reduce CO_2 emissions and carbon tax costs at the European level, highlighting their potential to drive the future of "Green Networks".

Keywords: 6 G, Green, Power consumption, Renewable energy, Optimization

1 Introduction

According to the ITU's IMT-2030 framework, anticipated applications for 6 G networks include immersive media experiences, multisensory interactions, digital twin technology, virtual environments, smart industry solutions, digital health innovations, and seamless integration of sensing with communication. Additionally, 6 G aims to support pervasive connectivity, enhanced intelligence, and advanced computing capabilities [1].

A key enabler of 6 G is the *ultra-densification* of networks through the deployment of numerous lightweight microbase stations (μBSs) [2]. These μBSs play a crucial role in dense network architectures by enhancing coverage and capacity in high-demand urban areas. By offloading traffic from macro base stations, they improve signal quality

Springer

and overall network efficiency [3]. Millimeter-wave (mmWave) bands[1] are key enablers of 6 G networks due to their ability to support extremely high data rates and large bandwidths, critical for future ultra-dense deployments. These high-frequency bands are especially relevant for urban deployments, where μBS densities are high. While mmWave signals suffer from high path loss and are more sensitive to blockage, these limitations are mitigated by the dense placement of μBSs [4]. Moreover, the short-range nature of mmWave aligns well with small cell infrastructure, making it ideal for the μ BS-based architectures considered in this work.

However, as the capabilities of 6 G networks expand, so do the challenges associated with energy consumption. The exponential growth in data traffic demands of future networks like 6 G raises challenges about related energy consumption and its environmental consequences.

1.1 Motivation: Why is energy efficiency more important in 6 G networks?

Energy consumption reduction is paramount in 6 G networks due to several pressing factors that shape the future of telecommunications infrastructure [5, 6]. With concerns about climate change and sustainability at the forefront of global consciousness, the need to reduce energy consumption in all sectors, including telecommunications, is more critical than ever. The information and communication technology (ICT) sector is projected to consume 20% of global energy by 2040 [7]. Additionally, in its 2019 report, the GSMA estimates that cellular networks contribute approximately 220 $MtCO_2$ annually to global emissions, a figure that could potentially double by 2025 [8]. Moreover, the deployment of 6 G networks is expected to involve a massive increase in the number of connected devices and infrastructure elements, from small cells to massive MIMO antennas, leading to a corresponding surge in energy needs. Therefore, optimizing energy efficiency in 6 G networks is essential to mitigate the environmental impact, reduce operational costs for service providers, and ensure the sustainability of future telecommunications infrastructure. BSs alone account for 80% of the total power consumption of the network, with their power consumption cost comprising about 15% of the network Opex [2, 9]. This emphasizes the significance of focusing on BS power consumption reduction.

In response to these challenges, there is a growing emphasis on incorporating renewable energy sources into the infrastructure of 6 G networks [10, 11]. The motivation behind this lies in the potential to reduce reliance on non-renewable energy sources, mitigate greenhouse gas emissions, help reduce the carbon footprint associated with fossil fuel-based energy generation, and enhance the overall sustainability of telecommunications infrastructure [12]. Renewable energy technologies such as solar, wind, and hydroelectric power offer a promising avenue for powering 6 G network operations in an environmentally friendly manner. By harnessing the abundant and renewable resources available, it becomes possible to optimize the power consumption of 6 G networks while simultaneously advancing toward a greener and more sustainable future [13, 14].

[1] mmWave ranges are between 24 and 300 GHz, including 5 G FR2 bands.

μBSs dynamically on/off switching (also called μBS sleep control) is widely regarded as a practical approach for saving energy and enhancing energy efficiency [12]. This technique allows μBSs to alternate between active and sleep modes to decrease power consumption during periods of low traffic demand while maintaining network coverage [14].

In parallel, emerging paradigms such as fluid antenna systems [15], RIS robustness under faulty elements [16], and integrated over-the-air computation with NOMA [17] broaden the 6 G design space, with implications for energy-efficient architectures and user association.

In this work, our primary goal is to reduce the grid power consumption of the network by integrating renewable energy sources through energy harvesting and implementing an intelligent dynamic switching mechanism that activates μBSs powered by renewable energy sources while deactivating those dependent on non-renewable (grid-based) energy whenever possible. We assume that grid power refers to electricity obtained from non-renewable sources (e.g., fossil fuel-based generation), in contrast to locally harvested solar or wind energy. Figure 1 illustrates the considered network scenario, highlighting the two types of μBSs. Green μBSs are powered by renewable energy, while red μ BSs rely on grid (non-renewable) power. In the depicted setup, user connections are prioritized toward renewable-powered μBSs, and most grid-powered μBSs are deactivated to reduce grid energy consumption. Only a few users are assigned to grid-powered μBSs when necessary.

1.2 Paper contributions

The main contributions of this paper are as follows:

- We formulated an optimization problem aimed at minimizing the power consumption of 5 G/6 G mmWave networks. This is achieved by maximizing the

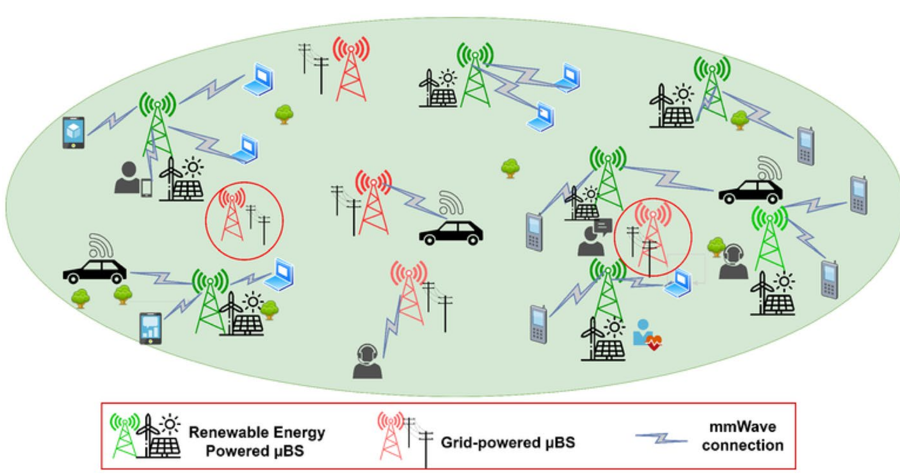

Fig. 1 Example of the network deployment with renewable and non-renewable energy sources. This figure shows the considered 6 G network scenario with two types of microbase stations (μBSs). Green μBSs are powered by renewable energy, while red μBSs rely on grid (non-renewable) power. User connections are preferentially directed to renewable-powered μBSs, while grid-powered μBSs are switched off whenever possible. Only a minimal number of users are assigned to grid-powered μBSs to reduce energy consumption

utilization of μBSs that are powered by renewable energy sources and deactivating those that rely on grid power. The goal is to drive the network toward deactivating as many grid-powered μBSs as possible, thus reducing overall power consumption and making the most of locally harvested energy. When it becomes necessary to activate a μBS powered by the grid, we minimize the number of users connected to that μBS, adhering to a load-based power consumption model.
- Given the NP-hard nature of the problem, solving the ILP for larger instances can be computationally intensive and time-consuming. To address this, we proposed three heuristic algorithms: the greedy green user allocation strategy (GUAS), the random user allocation strategy (RUAS), and the sequential user allocation strategy (SUAS). These algorithms are designed to efficiently solve larger-scale problems.
- Finally, we validated our proposed solutions through extensive simulations, evaluating their performance across various network sizes and user densities.

The rest of the paper is organized as follows: Sect. 2 reviews the prior work. Section 3 presents the problem formulation, system model, and the proposed solutions. Section 4 presents the simulation setup and the discussion of the results. Finally, Sect. 5 concludes the paper.

2 Related works

Recent research on sustainable 5 G/6 G networks has focused on integrating renewable energy and optimizing μBS on/off switching to improve energy efficiency.

Early studies such as [18] proposed hybrid-powered C-RAN models to reduce grid consumption, while Yang et al. [19] introduced a carbon-aware scheme using MILP to dynamically switch SBSs based on renewable availability. El Amine et al. [20] addressed battery aging in hybrid networks with a cost-aware BAPA algorithm. Al-Haj Hassan et al. [21] optimized grid power usage using utility-based traffic modeling, achieving notable energy savings.

Game-theoretic approaches like [22] tackled joint optimization of 5 G networks and smart grids, while other works, such as [23], used dynamic programming for BS scheduling. In the massive MIMO context, [24] proposed energy-efficient resource allocation for hybrid energy harvesting systems. For IoT scenarios, Wang et al. [25] introduced a fuzzy logic-based wakeup strategy to balance energy consumption and handoffs.

In our prior work [26], we proposed ILP and genetic algorithm-based solutions to reduce power consumption in mmWave networks via BS on/off switching. Our studies in [27, 28] explored user connectivity levels in mmWave systems, showing trade-offs between robustness and energy usage. Although the current work focuses on single-connectivity for tractability, our proposed framework can be extended to multiconnectivity scenarios.

To highlight our contribution in context, Table 1 compares key features across related studies.

Despite substantial progress, existing research lacks a comprehensive approach that maximizes renewable-powered BS usage while minimizing grid-powered activity based on load. Our work addresses this gap through a load-based power model that selectively

Table 1 Comparison of related works with our proposed framework

Work	Grid-power minimization	Load-based user association	BS ON/OFF switching	Renewable integration	Heuristic solutions
[18]	✓	×	×	✓	×
[19]	✓	×	✓	✓	×
[20]	✓	×	✓	✓	×
[21]	✓	×	×	✓	×
[22]	✓	×	×	✓	×
[23]	✓	×	✓	✓	✓
[24]	✓	×	×	✓	✓
[25]	✓	×	✓	✓	✓
[26–28]	✓	×	✓	×	✓
This	✓	✓	✓	✓	✓

activates grid-powered BSs only when necessary, significantly reducing overall grid energy consumption.

3 Methods and experimental setup

3.1 System model

Let S denote the set of all μBSs uniformly distributed in an area of size A. We define $S_1 \subset S$ as the subset of μBSs powered by renewable energy, where the number of renewable μBSs is given by $|S_1| = \lfloor \eta \cdot |S| \rfloor$, and $\eta \in [0, 1]$ represents the renewable energy penetration ratio. The remaining μBSs belong to the set S_2, which are powered by the grid, such that $S = S_1 \cup S_2$ and $S_1 \cap S_2 = \emptyset$. Accordingly, the total number of grid-powered stations is $|S_2| = |S| - |S_1|$. To focus on the core user association and μBS on/off switching logic, we assume that renewable-powered μBSs are equipped with batteries of sufficient capacity to support typical off-sunlight operation (e.g., overnight). This assumption is supported by the increasing availability of high-capacity, low-cost energy storage technologies being co-deployed with solar infrastructure in telecom applications [29]. This assumption simplifies the model to focus on spatial optimization. In future work, we aim to integrate time-dependent energy harvesting profiles, battery constraints, and charging dynamics for a more realistic representation. We assume that the grid-power consumption μBS equals 0 W if that μBS $\in S_1$. Additionally, we have a set of users U uniformly distributed in the area. An illustrative example is shown in Fig. 2, where each red diamond represents a μBS powered by electricity from the grid, each yellow "X" represents a μBS powered by a renewable energy source, and the blue plus represents the end user.

The primary objective of this study is to minimize the power consumption of the networks from the grid and maximize the dependability of the network on the power provided by renewable energy systems while maintaining user QoS. We refer to this as the ***User Allocation with Green Power Maximization*** problem.

3.2 Power consumption model of μBSs

We consider the *Load-based linear* power model, where the power consumption of the μBS is directly proportional to the number of users connected to it (referred to as the load of the μBS). In contrast, the *Stepwise* power model presented in [28, 30] operates under two

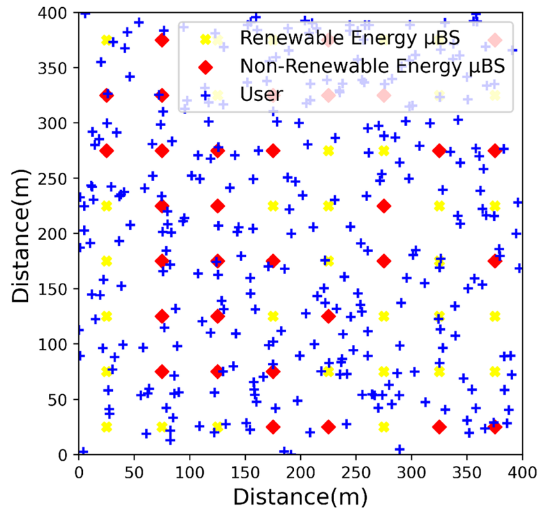

Fig. 2 Users and μBSs distribution for 400 users and 50% renewable energy. This figure illustrates the distribution of users (blue plus symbols) and μBSs in a 400 m x 400 m area, with 400 users and 50% of μ BSs powered by renewable energy. Red diamonds denote grid-powered μBSs, yellow crosses represent renewable-powered μBSs, and blue plus symbols indicate users. The figure highlights how users are spatially distributed relative to the available μBSs

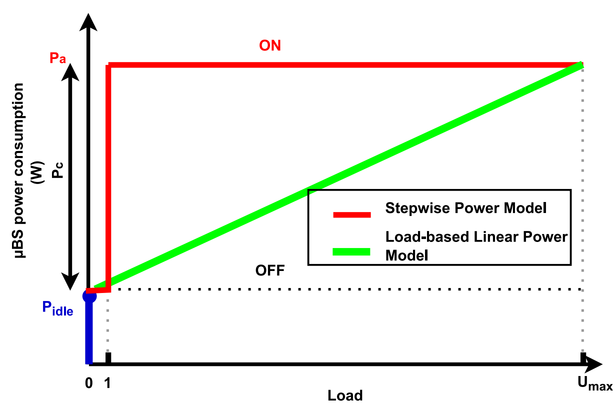

Fig. 3 μBS power consumption models. This figure compares the stepwise power model and the load-based linear power model. In the stepwise model, a μBS consumes maximum power when at least one user is connected and idle power when no users are connected. In the load-based linear model, power consumption increases proportionally with the number of connected users, offering finer energy adaptation

conditions: The μBS is either on if at least one user is connected to it (requiring maximum power consumption regardless of the load) or off if there are no users connected to it. In the case of *Load-based linear* power model, we can calculate P_{cs} of the μBS as follows:

$$P_{cs} = P_{\text{idle}} + P_n \cdot \left(\frac{\sum_{s \in S} x_{us}}{|U_{\max}|} \right), \quad \forall u \in U \tag{1}$$

where P_n, is the difference between P_a and P_{idle}, as will be shown later. x_{us} is a binary variable which determines if user u is connected to μBS s, as further detailed in Section

III, Subsection D. While in the *Stepwise* power model [27], P_c either equals P_a when it is on or P_{idle} when it is off, as shown in Fig. 3.

Note: In this study, each μBS is assumed to be an omnidirectional single cell, so there is no possibility to partially turn off a base station.

3.3 Channel model and data rate

In this study, we consider large-scale path loss and shadowing effects using the floating intercept path loss model and lognormal variability, as commonly used in mmWave modeling [31]. We omit fast fading and user mobility effects to focus on spatial user association and base station switching strategies under stable topology conditions. Incorporating time-varying channel characteristics and user mobility would require a cross-layer optimization framework, which we plan to explore in future work. The path loss model is given by:

$$L(d) = L(d_0) + \eta 10 \log_{10}(d) + \xi, \quad \xi \sim N(0, \sigma^2) \tag{2}$$

where

$$L(d_0) = 20 \log_{10}\left(\frac{4\pi d_0}{\lambda}\right), \tag{3}$$

where $L(d_0)$ is the path loss in decibels (dB) at a reference distance of d_0 meters between the transmitter and the receiver, η is the least square fits of the floating intercept and slope over the measured distances up to 200 m, σ^2 is the variance of the lognormal shadowing, ξ represents a normally distributed random variable with mean 0 and variance σ^2, and λ is the wavelength.

The received signal power P_{rx}^{su} for a given user equipment u UE at distance d from a given μBS s can be calculated using the expression:

$$P_{rx}^{su} = P_{tx}^{su} + G_{tx} - L(d) + G_{rx}, \tag{4}$$

where P_{tx}^{su} is the transmitted power from μBS s to UE u, and G_{tx} and G_{rx} are the gains of the transmitter and receiver antennas, respectively. The antenna gain can be calculated as follows:

$$G = 20 \log_{10}\left(\frac{\pi \cdot l}{\lambda}\right), \tag{5}$$

where l is the antenna length, either for the μBS or the UE. While λ is the wavelength based on the used frequency. The transmission power P_{tx}^{su} from μBS s to UE u must satisfy the power constraint.

$$\sum_{u \in U} P_{tx}^{su} \leq P_{max,s}, \tag{6}$$

where $P_{max,s}$ is the maximum RF output power of μBS s at its maximum traffic load. The *signal-to-interference-plus-noise ratio* (SINR) for user u ($u \in U$) from μBS s ($s \in S$) is given by

$$\mathrm{SINR}_{su} = \frac{P_{su}^{rx}}{I_s + P_{\mathrm{noise}}} \tag{7}$$

where I_s is the inter-cell interference and P_{noise} is the additive white Gaussian noise power. The interference I_s caused by other μBSs can be calculated as

$$I_s = \sum_{n \in S, n \neq s} \frac{P_{tx}^{nu}}{L(d_{nu})} \tag{8}$$

The additive white Gaussian noise power P_{noise} is calculated as:

$$P_{\mathrm{noise}} = -174 + 10\log_{10}(B) \tag{9}$$

where B is the bandwidth in Hertz (Hz).

Although mmWave networks are generally considered noise-limited due to highly directional transmissions and sensitivity to blockages, ultra-dense deployments can still experience residual inter-cell interference. Factors such as imperfect beam alignment, side-lobe leakage, and beam collisions can contribute to non-negligible interference. Therefore, we conservatively include the interference term I_s in our SINR model to account for these effects. This approach ensures robustness in highly dense scenarios, even if the overall interference level remains low compared to thermal noise in typical settings.

Note: Since our focus was on investigating on/off switching and having the above-described linear power model, we assume a simplified model where each microbase station is equipped with a single omnidirectional dipole antenna. This results in inter-cell interference, which may still be significant in dense deployments. Therefore, we explore both interference- and noise-limited regimes in a separate analysis presented in Sect. 4.

We analyze both interference-limited and noise-dominated regimes. By default, with single dipole omnidirectional antennas, the network may operate in an interference-limited regime under high spatial reuse. To reflect the transition to directional isolation with beamforming, we introduce an interference scaling factor that attenuates inter-cell interference by 0 dB, −10 dB, −20 dB, and −30 dB, illustrating how the system becomes effectively noise-limited as directionality increases (cf. Section 4.3). This makes our results comparable under both omnidirectional and directional scenarios.

According to Shannon's capacity formula, we can determine the maximum achievable throughput (data rate) R_{su} for user u from μBS s as follows:

$$R_{su} = B \cdot \log_2(1 + \mathrm{SINR_{su}}). \tag{10}$$

Note: All logarithmic expressions (path loss, antenna gain) are in dB. Transmit and receive powers are handled consistently: dBm for RF power levels; linear units for SINR calculation.

3.4 ILP formulation

The input parameters are defined as follows:

- P_a: The maximum power consumed by the μBS when active and fully loaded.

- P_c: The power consumed by the µBS when active.
- P_{idle}: Power consumed by the µBS when inactive.
- P_n: The difference between P_a and P_{idle}, ($P_n = P_a - P_{\text{idle}}$).
- K: Large number (i.e., 1000) (this value was chosen experimentally). We set K = 1000 to dominate P_c terms while avoiding numerical instability in the solver. Tests with K ∈ 100, 500, 1000, 5000 produced identical optimal solutions, with K = 1000 yielding stable solving times.
- U: Set of users (where $|U|$ is the total number of users).
- S: Set of μBSs (where $|S|$ is the total number of μBSs).
- $d_{\max}$: Maximum allowed distance between the user and the µBS.
- $\text{Th}_{\min}$: Minimum throughput threshold required for each user.
- $U_{\max}$: Maximum number of users that can be allocated to one µBS.
- $P_{\max}$: Maximum transmitted power of the µBS.
- R_{us}: The data rate allocated each user u from µBS s.

Decision variables are defined as follows:

- x_{us} is a binary variable that equals 1 if user u is assigned to µBS s, and 0 otherwise. The user-to-µBS association is represented by matrix $X = [x_{us}]$ of size $|U| \times |S|$.
- y_s is a binary variable that equals 1 if µBS s is active, and 0 if it is in sleep (idle) mode.

Objective function:

$$\text{Minimize} \sum_{s \in S_2} (K \cdot y_s \cdot P_c + (1 - y_s) \cdot P_{\text{idle}}) - \sum_{s \in S_1} y_s \tag{11}$$

The term $-\sum_{s \in S_1} y_s$ in the objective function acts as a penalty-reduction mechanism, incentivizing the model to prioritize the activation of renewable-powered base stations to maximize green energy utilization.

Subject to:

$$\sum_{s \in S} x_{us} = 1, \quad \forall u \in U \tag{12}$$

$$y_s \geq x_{us}, \quad \forall u \in U, s \in S_2 \tag{13}$$

$$\sum_{s \in S} x_{us} \geq y_s, \quad \forall s \in S_2 \tag{14}$$

$$\sum_{u \in U} x_{us} \leq U_{\max}, \quad \forall s \in S \tag{15}$$

$$\sum_{u \in U} x_{us} \cdot P_{tx}^{su} \leq P_{\max}, \quad \forall s \in S \tag{16}$$

$$R_{us} \geq \mathrm{Th}_{\min} \cdot \mathrm{x_{us}}, \quad \forall \mathrm{u} \in \mathrm{U}, \mathrm{s} \in \mathrm{S} \tag{17}$$

$$x_{us} \cdot d_{us} \leq d_{\max}, \quad \forall u \in U, s \in S \tag{18}$$

$$x_{us}, y_s \in \{0, 1\} \quad \forall u \in U, s \in S \tag{19}$$

Constraint 12 indicates that the user can be assigned to one grid-powered μBS only. Constraint 13 ensures that the grid-powered μBS must be activated if at least one user is assigned to it. Constraint 14 ensures that the μBS is switched off if no users are assigned to it (this constraint can be relaxed as it is included in the objective function). Constraint 15 ensures that the maximum number of users assigned to a µBS must not exceed $U_{\max}$, the maximum number of connections per μBS. Constraint 16 shows that the total transmission power must not exceed the maximum value $P_{\max}$ of the μ BS. Constraint 17 indicates that the data rate R_{uq} allocated to each user must be at least equal to the minimum threshold $\mathrm{Th}_{\min}$. Constraint 18 ensures that the distance d_{us} between user u and μBS s must not exceed the maximum allowed distance $d_{\max}$. Finally, Constraint 19 indicated that the used variables are binary.

3.5 Proof of NP-hardness

1 Theorem

The problem of User Association with Green Power Maximization (Eqs. 11–19) is NP-hard.

1 *Proof*

We prove NP-hardness by a polynomial-time reduction from the classic Set Cover Problem (SCP), which is known to be NP-hard [32]. □

3.5.1 Set cover problem (SCP)

SCP is defined as follows:

- **Input:** A universe U and a collection $\mathcal{S}$ of subsets of U, each with an associated cost.
- **Goal:** Select a minimum-cost subcollection $\mathcal{S}' \subseteq \mathcal{S}$ such that every element in U is covered.

3.5.2 Reduction to the ILP problem

We construct a special case of our ILP to mirror SCP:

- Each element $u \in U$ maps to a user in our ILP.
- Each subset $S_i \in \mathcal{S}$ maps to a μBS $s \in S$.
- Assigning user u to μBS s ($x_{us} = 1$) corresponds to $u \in S_i$ in SCP.

- Activating a μBS ($y_s = 1$) incurs a cost analogous to selecting a subset.

Under simplified assumptions (e.g., $P_c = 1$, $P_{\text{idle}} = 0$, and constraints on distance, throughput, etc., are trivially satisfied), the ILP reduces to finding the minimum number of μBSs that can serve all users—directly analogous to SCP.

Since SCP is NP-hard and can be reduced to our ILP in polynomial time, our problem is also **NP-hard**.

3.6 Heuristic solutions

3.6.1 Why multiple heuristics?

Given the NP-hard nature of the problem and the diverse conditions in real-world 6 G scenarios (e.g., dynamic user distributions, non-uniform μBS types), we propose three distinct heuristics—GUAS, RUAS, and SUAS. Each serves a complementary purpose:

1. GUAS (Greedy Green User Allocation Strategy) seeks energy efficiency by prioritizing renewable μBSs and applying iterative grid μBS optimization.
2. RUAS (Random User Allocation Strategy) introduces stochasticity to explore broader allocation possibilities and serves as a randomized baseline.
3. SUAS (Sequential User Allocation Strategy) provides a simple, deterministic method that reflects a distance-prioritized connection logic.

The combination allows us to evaluate solution robustness and trade-offs in energy savings versus algorithmic complexity. Each is described in detail below.

3.6.2 Greedy green user allocation strategy (GUAS)

The pseudo-code provided in Algorithm 1 outlines an algorithm to optimize user connections to μBSs in a system with both solar-powered (S_1) and grid-powered (S_2) μ BSs. This algorithm seeks to allocate users to μBSs in a way that minimizes grid-based power usage, particularly by applying multiple iterations to identify the most power-efficient configurations for S_2. The algorithm consists of the following main steps:

1. **Initial Setup:** The algorithm divides the available μBSs into two sets:

   - S_1: Set of solar-powered μBSs.
   - S_2: Set of grid-powered μBSs.

   The total power consumption is initially set to infinity ($P_{\text{best}} \leftarrow \infty$), and placeholders are established for the best connection configuration (‘best_connections‘) and the best power distribution (‘best_power_distribution‘).

2. **Assigning Users to Solar-Powered μBSs** (S_1): For each user u in the set of users U, the algorithm first tries to assign u to a μBS in S_1 based on certain conditions:

   - The distance between the user and the μBS is within a maximum allowable distance $D_{\max}$.

- The signal-to-interference-plus-noise ratio (SINR) between the user and the μBS exceeds a minimum threshold R_{min}.
- The number of users connected to the μBS does not exceed the maximum allowable connections U_{max}.

Among the μBSs in S_1 that meet these conditions, the μBS with the highest SINR is selected for each user to maximize signal quality. This step helps to minimize power consumption by prioritizing solar-powered μBSs, reducing dependence on grid-powered stations.

3. **Iterative Optimization for Grid-Powered μBSs** (S_2): The algorithm then performs a series of $N_{\text{iterations}}$ iterations ($N_{\text{iterations}}$=50, this value was chosen experimentally where the algorithm converges. We measured convergence by tracking successive improvements in grid power and observed diminishing returns beyond 40–60 iterations. The value of 50 iterations balances solution quality and runtime (no improvement beyond 50).) to optimize the configuration of connections to grid-powered μBSs (S_2). In each iteration, the algorithm attempts different configurations for connecting users who were not assigned to any solar-powered μBS in S_1. For each user without a connection:

- It evaluates each μBS in S_2 based on the same distance, SINR, and connection limit criteria used for S_1.
- The first valid μBS from S_2 that meets these conditions is selected for each user.

After assigning users to S_2 μBSs in each iteration, the algorithm calculates the total power consumption for the current configuration. This calculation considers the idle and active power requirements of each grid-powered μBS:

- If no users are connected to a μBS, its power consumption is set to P_{idle}.
- Otherwise, the power consumption is calculated as $P_{\text{idle}} + \left(\frac{\text{connected\_users}(\mu\text{BS})}{U_{\text{max}}}\right) \cdot P_{\text{n}}$.

4. **Updating the Best Solution:** If the total power consumption for the current iteration is lower than the previous best (P_{best}), the algorithm updates the best solution with the current configuration of connections and power distribution. This ensures that, by the end of all iterations, the algorithm has identified the configuration for S_2 connections with the lowest power consumption.
5. **Return** The algorithm returns the best configuration of connections (‘best_connections‘), the power distribution across μBSs (‘best_power_distribution‘), and the total minimized power consumption (P_{best}).

Algorithm 1 Greedy Green User Allocation Strategy (GUAS)

```
procedure Optimize Grid power consumption with user assignment(S, U, D_max, R_min, U_max, P_idle, P_n, N_iterations)
    S_1 ← μBSs powered by renewable (solar)sources
    S_2 ← μBSs powered by the grid
    P_best ← ∞                                          ▷ Initialize best power consumption to infinity
    best_connections ← ∅                                ▷ Initialize best solution connections
    best_power_distribution ← ∅                         ▷ Initialize best power distribution
    for u in U do                                       ▷ First, connect each user to solar-powered μBSs if possible
        μBS_selected ← None
        SINR_max ← 0
        for μ BS in S_1 do
            if distance(u, μBS) ≤ D_max and SINR(u, μBS) > R_min and connected_users(μBS) < U_max then
                if SINR(u, μBS) > SINR_max then
                    SINR_max ← SINR(u, μBS)
                    μBS_selected ← μBS
                end if
            end if
        end for
        if μBS_selected ≠ None then
            connect_user(u, μBS_selected)
        end if
    end for
    for i = 1 to N_iterations do                        ▷ Iterate for optimal grid-powered μBS connections
        P_total ← 0
        current_connections ← ∅
        current_power_distribution ← ∅
        for u in U do
            if user_connected(u) = False then           ▷ Only assign users not already connected to S_1
                μBS_selected ← None
                for μBS in S_2 do                       ▷ Check grid-powered stations in each iteration
                    if distance(u, μBS) ≤ D_max and SINR(u, μBS) > R_min and connected_users(μBS) < U_max then
                        μBS_selected ← μBS
                        break                           ▷ Assign the first valid μBS from S_2 in this iteration
                    end if
                end for
                if μBS_selected ≠ None then
                    connect_user(u, μBS_selected)
                    current_connections[u] ← μBS_selected
                end if
            end if
        end for
        for μBS in S_2 do                               ▷ Calculate power for grid-powered stations
            if connected_users(μBS) = 0 then
                power_consumption(μBS) ← P_idle
            else
                power_consumption(μBS) ← P_idle + (connected_users(μBS) / U_max) · P_n
            end if
            P_total ← P_total + power_consumption(μBS)
            current_power_distribution[μBS] ← power_consumption(μBS)
        end for
        if P_total < P_best then                        ▷ Update the best solution if current power is lower
            P_best ← P_total
            best_connections ← current_connections
            best_power_distribution ← current_power_distribution
        end if
    end for
    return best_connections, best_power_distribution, P_best
end procedure
```

3.6.3 *Random user allocation strategy (RUAS)*

RUAS is designed to allocate users to μBSs in a network powered by renewable (solar) and grid-based energy sources. The algorithm randomly assigns users to available μ BSs using an iterative approach to explore different random allocations of users to μBSs over multiple trials while considering constraints such as distance, signal quality, and μBS capacity. It ensures users are connected only if a valid connection is feasible. It then calculates power consumption based on the number of users connected to each μBS, focusing on minimizing grid-power usage while maintaining service quality. Algorithm 2 proceeds as follows:

- **Input Parameters**: The algorithm receives as input a set of µBSs S, a set of users U, a maximum connection distance D_{max}, a minimum SINR threshold R_{min}, a maximum user capacity per µBS U_{max}, and two power parameters: the idle power P_{idle} and the maximum power consumption P_{max} for each µBS.
- **Initialization**: The µBSs are divided into two subsets: S_1, consisting of µBSs powered by solar energy, and S_2, consisting of those powered by the grid. A variable P_{best} is initialized to infinity to store the minimum power consumption found across all iterations. Additionally, empty sets are prepared to store the best configurations of user connections and µBS power distributions.
- **Iterative Random Assignment**: The algorithm performs $N_{\mathrm{iterations}}$ trials, where each iteration involves the following steps:
  - For each user $u \in U$, a µBS $\mu\mathrm{BS}_{\mathrm{selected}}$ is randomly selected from S. The algorithm then checks whether this random µBS meets three conditions: (1) The user is within D_{max} of the µBS, (2) the SINR between the user and µBS exceeds R_{min}, and (3) the µBS has capacity available to connect an additional user (i.e., connected users $< U_{\mathrm{max}}$). If these conditions are met, the user is connected to $\mu\mathrm{BS}_{\mathrm{selected}}$.
- **Power Consumption Calculation for Grid-Powered Stations**: After all users have been assigned in the current iteration, the algorithm calculates the power consumption for each grid-powered µBS in S_2:
  - If a µBS has no connected users, its power consumption is set to P_{idle}.
  - Otherwise, the power consumption is computed as

    $$P_{\mathrm{idle}} + \left(\frac{\mathrm{connected\_users}(\mu\mathrm{BS})}{U_{\mathrm{max}}}\right) \cdot P_{\mathrm{n}},$$

    where P_{n} represents the proportional increase in power based on the load on the µBS.

    The total power consumption P_{total} for the current iteration is computed as the sum of the power consumptions of all grid-powered µBSs in S_2.
- **Best Solution Update**: If the total power consumption P_{total} for the current iteration is less than the current best power consumption P_{best}, then P_{best} is updated with P_{total}, and the configurations of user connections and power distributions are stored as the best solution found so far.
- **Return Optimal Solution**: After completing all iterations, the algorithm returns the best user connections, power distribution, and total power consumption recorded across all iterations. This final configuration represents the allocation with the lowest observed power consumption.

Algorithm 2 Random User Allocation Strategy (RUAS)

```
procedure RANDOM ALLOCATION(S, U, D_max, R_min, U_max, P_idle, P_n, N_iterations)
    S_1
    S_2
    P_best ← ∞
    best_connections ← ∅
    best_power_distribution ← ∅
    for i = 1 to N_iterations do
        P_total ← 0
        current_connections ← ∅
        current_power_distribution ← ∅
        for u in U do                    ▷ Randomly assign each user in each iteration
            μBS_selected ← randomly_select(S)
            if distance(u, μBS_selected) ≤ D_max and SINR(u, μBS_selected) > R_min
and connected_users(BS_selected) < U_max then
                connect_user(u, μBS_selected)
                current_connections[u] ← μBS_selected
            end if
        end for
        for μBS in S_2 do                ▷ Calculate power for grid-powered stations
            if connected_users(μBS) = 0 then
                power_consumption(μBS) ← P_idle
            else
                power_consumption(μBS) ← P_idle + (connected_users(μBS) / U_max) · P_n
            end if
            P_total ← P_total + power_consumption(μBS)
            current_power_distribution[μBS] ← power_consumption(μBS)
        end for
        if P_total < P_best then ▷ Update the best solution if current power is lower
            P_best ← P_total
            best_connections ← current_connections
            best_power_distribution ← current_power_distribution
        end if
    end for
    return best_connections, best_power_distribution, P_best
end procedure

function RANDOMLY_SELECT(S)
    index ← random integer between 0 and length(S) − 1
    return S[index]
end function
```

3.6.4 Sequential user allocation strategy (SUAS)

SUAS is a method for connecting users to μBSs in a sequential manner. Unlike the RUAS, which randomly assigns users to μBSs, SUAS systematically assigns users to the μBSs in the order of their distance from the 0 point in the set S. The algorithm checks each μBS one by one and connects users only if the conditions related to distance, signal quality, and capacity are satisfied.

The step-by-step explanation of the pseudo-code in Algorithm 3 is as follows:

1. **Initialize the Sets:** The algorithm begins by categorizing μBSs into S_1, the solar-powered stations, and S_2, the grid-powered stations. It also initializes a variable P_{total} to keep track of the total power consumption of grid-powered μBSs.
2. **User Allocation:** For each user $u \in U$, the algorithm selects the next μBS in S sequentially. This selection is performed by the helper function NEXT_BASE_STATION, which returns the next μBS in the order of S. The algorithm verifies that the selected μBS meets three conditions:

   - The distance between the user u and the μBS $\mu\text{BS}_{\text{selected}}$ does not exceed $D_{\max}$.
   - The SINR between u and $\mu\text{BS}_{\text{selected}}$ is greater than or equal to the minimum threshold $R_{\min}$.
   - The number of users currently connected to $\mu\text{BS}_{\text{selected}}$ is less than $U_{\max}$.

   If any of these conditions are not met, the algorithm moves to the next μBS in S and repeats the check until it either finds a suitable station or exhausts the list of stations. If the list is exhausted, no connection is established for that user.

3. **Connection to μBS:** If a μBS $\mu\text{BS}_{\text{selected}}$ meeting all conditions is found, the user is connected to that μBS using the CONNECT_USER function.
4. **Power Consumption Calculation for Grid-Powered Stations:** After all users have been allocated, the algorithm calculates power consumption for each grid-powered μBS $\mu\text{BS} \in S_2$. For each μBS in S_2:

   - If there are no connected users, the power consumption is set to zero.
   - Otherwise, the power consumption is calculated as:

   $$P_{\text{idle}} + \left(\frac{\text{connected\_users}(\mu\text{BS})}{U_{\max}}\right) \cdot P_{\text{n}}$$

   This calculated power consumption for each station is then added to P_{total}.
5. **Return Results:** The algorithm concludes by returning the final list of connected users, the power consumption of each μBS, and the total power consumption P_{total} for grid-powered stations.

Algorithm 3 Sequential User Allocation Strategy (SUAS)

procedure SEQUENTIAL ALLOCATION($S, U, D_{\max}, R_{\min}, U_{\max}, P_{\text{idle}}, P_{\max}$)
    S_1
    S_2
    $P_{\text{total}} \leftarrow 0$
    for u **in** U **do**
        $\mu\text{BS}_{\text{selected}} \leftarrow \text{next\_base\_station}(S)$ ▷ Start with the first µBS in S
        while $\text{distance}(u, \mu\text{BS}_{\text{selected}}) > D_{\max}$ **or** $\text{SINR}(u, \mu\text{BS}_{\text{selected}}) < R_{\min}$ **or** $\text{connected\_users}(\mu\text{BS}_{\text{selected}}) \geq U_{\max}$ **do**
            $\mu\text{BS}_{\text{selected}} \leftarrow \text{next\_base\_station}(S)$ ▷ Move to the next µBS in sequence
            if $\mu\text{BS}_{\text{selected}} = \text{None}$ **then** ▷ End of S reached without finding a suitable µBS
                break ▷ No suitable µBS, break loop for this user
            end if
        end while
        if $\mu\text{BS}_{\text{selected}} \neq \text{None}$ **then**
            $\text{connect\_user}(u, \mu\text{BS}_{\text{selected}})$
        end if
    end for
    for BS **in** S_2 **do** ▷ Calculate power only for grid-powered stations
        if $\text{connected\_users}(\mu\text{BS}) = 0$ **then**
            $\text{power\_consumption}(\mu\text{BS}) \leftarrow P_{\text{idle}}$
        else
            $\text{power\_consumption}(\mu\text{BS}) \leftarrow P_{\text{idle}} + \left(\frac{\text{connected\_users}(\mu\text{BS})}{U_{\max}}\right) \cdot P_{\text{n}}$
        end if
        $P_{\text{total}} \leftarrow P_{\text{total}} + \text{power\_consumption}(\mu\text{BS})$
    end for
    return $\text{connected\_users}(S), \text{power\_consumption}(S), P_{\text{total}}$
end procedure
function NEXT_BASE_STATION(S)
    return the next µBS in the order of S, or **None** if end of S is reached
end function

3.7 Summary of heuristic algorithms

The three proposed heuristics—GUAS, RUAS, and SUAS—are designed to provide scalable approximations to the ILP-based user association problem under renewable energy constraints. GUAS uses a deterministic SINR-based greedy strategy for renewable µBSs and iterative optimization for grid-powered µBSs. RUAS employs randomized user allocation across µBSs to explore diverse configurations. SUAS sequentially allocates users based on a fixed ordering of µBSs. These methods vary in complexity and allocation consistency, offering trade-offs between performance and computation time. Table 2 summarizes their core features.

4 Simulation results and discussion

In this section, we present and analyze the simulation results and observations. For simulation, we modeled a network consisting of multiple users and µBSs within a predefined area. The area size for the simulation was set to 400 m x 400 m, and the distance limit ($d_{\max}$) between any two nodes was 50 m. The number of users varied from 50 to 500, while the number of µBSs ($|S|$) remained fixed at 64. The network operates on a 28 GHz

Table 2 Summary of proposed heuristic algorithms

Algorithm	Main idea	Time complexity
GUAS	Greedy selection of best SINR renewable μBS; iterative refinement for grid μBSs	$\mathcal{O}(\lvert U\rvert\lvert S\rvert + N_{iter}\lvert S_2\rvert)$
RUAS	Random assignment of users to μBSs over multiple iterations	$\mathcal{O}(N_{iter} \cdot \lvert U\rvert\lvert S\rvert)$
SUAS	Sequential allocation of users based on μBS order	$\mathcal{O}(\lvert U\rvert\lvert S\rvert)$

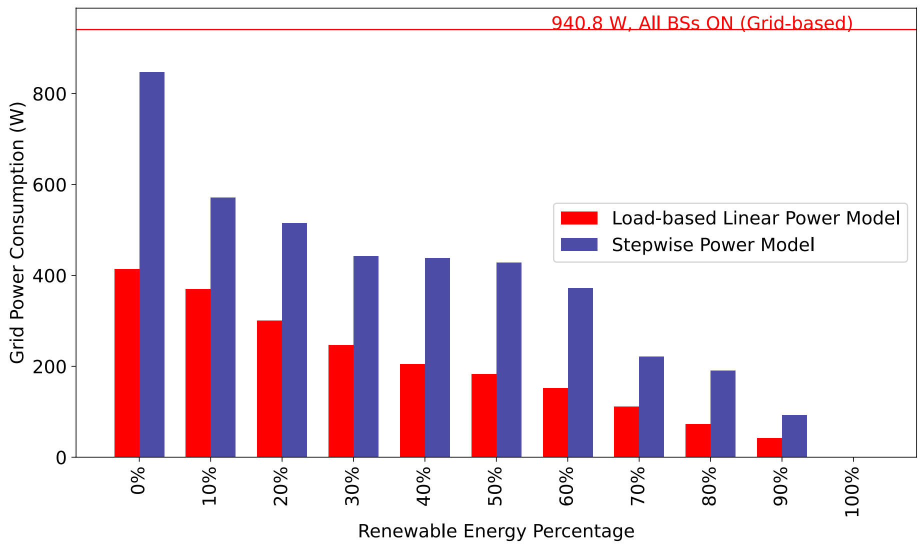

Fig. 4 Load-based linear vs. stepwise power model for 400 users. This figure compares grid-power consumption under the stepwise and load-based linear power models, as well as the baseline case where all μBSs are continuously active. For 400 users, the load-based linear model achieves the lowest power consumption, especially at higher renewable energy penetration levels. Results are averaged over 50 simulation runs

frequency band, with a bandwidth (B) of 1200 MHz. Path loss calculations were based on a reference distance (d_0) of 1 m, and the corresponding path loss at d_0 was $L(d_0) = 61.4$ dB calculated based on 3. The path loss exponent (η) was set to 2.1 [33]. Users' maximum transmit power ($P_{\max}$) was capped at 30 dBm, and the power variance (ξ) was set at 5.8 [33]. The wavelength of the signal (λ) was 10.7 mm. Additionally, the transmit and receive antenna lengths were $l(tx) = 0.1$ m and $l(rx) = 0.01$ m, respectively. Power consumption parameters included $P_a = 14.7$ W and $P_i = 4.3$ W [34]. The network can support up to $U_{\max} = 30$ users, with a minimum throughput ($\text{Th}_{\min}$) of 20 Mbps. Finally, the renewable energy percentage (η) was varied in increments of 25%, from 25% to 75%.

To determine the optimal solutions, we employed the commercially available CPLEX solver. The heuristic simulations were developed and carried out using the Python programming language.

4.1 Optimal on-grid-power consumption (stepwise vs. load-based linear model)

Figure 4 presents a comparative analysis of the stepwise power model, the load-based linear power model, and the scenario where all μBSs remain continuously active, taking into account that the number of users is 400. The results indicate that while the stepwise model achieves a notable reduction in power consumption compared to having all μBSs active—particularly in low-user density scenarios—it still demands up to 50% more power than the load-based approach. The results shown in the figure are an average of 50 experiments.

In Fig. 5, we illustrate the relationship between the percentage of renewable energy-powered μBSs and the corresponding power consumption from both renewable and non-renewable sources. As the percentage of renewable energy increases, the power consumption from non-renewable sources significantly decreases, starting at 413.86 W at 0% renewable energy and approaching zero at 100%. Conversely, the power consumption from renewable sources rises sharply, reaching a maximum of 940.8 W at 100% renewable energy. Interestingly, the total power consumption, represented by the blue line, exhibits an overall increase as the percentage of renewable energy rises.

However, this increase is offset by the reduction in non-renewable consumption, emphasizing that while total consumption rises compared to the 0% renewable scenario, it does not burden the electrical grid. The red dashed line at 940.8 W represents the total power consumption when all μBSs are powered by the grid, serving as a benchmark for evaluating the impact of grid/power μBSs switching on/off strategy with renewable integration. This analysis highlights that although total power consumption will increase, this rise is offset by renewable energy sources, which are considered free power for mobile network operators.

Additionally, Fig. 6 illustrates a comparative analysis between the stepwise power model and the load-based linear power model across varying user densities and renewable μBS percentages, ranging from 0% to 75% in 25% increments. The results demonstrate a substantial reduction in power consumption achieved by the load-based strategy. This significant improvement is especially evident in scenarios with higher percentages of renewable μBSs.

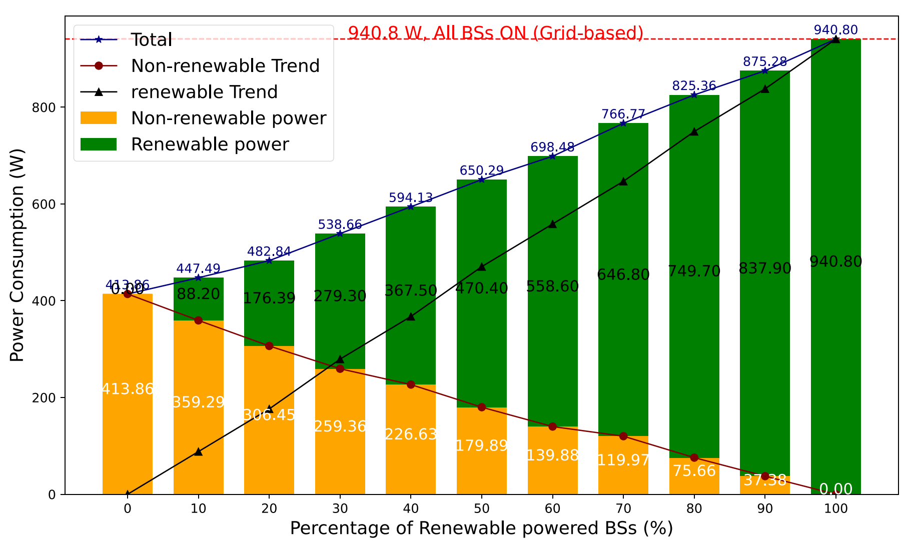

Fig. 5 Simulated network power consumption trend using renewable and grid-power sources. This figure shows total power consumption as renewable penetration increases from 0 to 100%. Non-renewable consumption decreases as renewable penetration rises, while renewable power consumption increases. Although total consumption grows, this increase is offset by renewable sources, reducing grid dependency

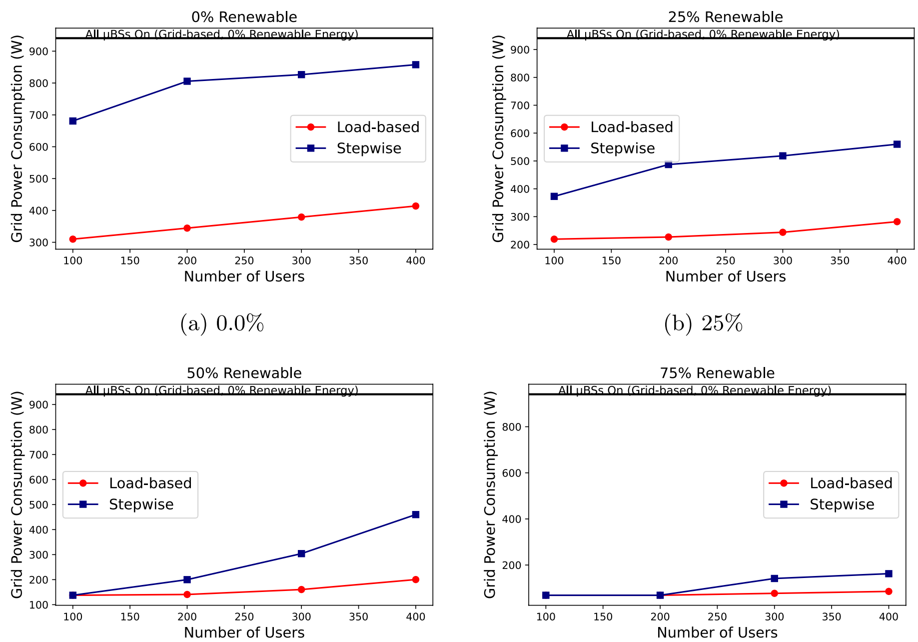

(a) 0.0% (b) 25%

(c) 50% (d) 75%

Fig. 6 Power consumption versus number of users for different renewable energy percentages. This multipanel figure **a**–**d** compares grid-power consumption under the stepwise and load-based linear models for 0%, 25%, 50%, and 75% renewable penetration. The load-based model consistently achieves greater reductions in grid-power usage, particularly at high-user densities

Table 3 Grid-power consumption reduction % compared to the case of all μBSs is always on and no renewable energy used, considering the stepwise and load-based linear power models for both, **'Low'** and **'High'** user densities

	Renewable energy %	**0%**	**25%**	**50%**	**75%**
Low	Load-based linear model	67.07	76.69	85.37	92.69
	Stepwise model	27.63	60.37	85.37	92.69
High	Load-based linear model	56.03	70.04	78.70	90.92
	Stepwise model	8.85	40.49	51.12	82.74

Table 3 summarizes the results from Fig. 6, comparing the grid-power consumption reduction achieved by two power models—load-based linear and stepwise—under varying levels of renewable energy integration (0%, 25%, 50%, and 75%). The analysis considers two scenarios: low user density (100 users) and high-user density (400 users). The table shows the percentage reduction in power consumption relative to a baseline scenario where all μBSs are always on, and no renewable energy is used.

The results demonstrate that the load-based linear power model consistently achieves greater reductions, particularly in high-user density scenarios, where efficient grid-powered μBS switching is essential to manage the large number of users. A similar trend is observed for low-user density scenarios with 0% or 25% renewable energy, as the limited availability of renewable energy emphasizes the efficiency of the load-based linear power model. However, for low-user density with 50% or 75% renewable energy, the reduction percentages for both power models converge. This is attributed to the increased availability of renewable energy, allowing more μBSs to be powered sustainably, switching off the grid-powered μBSs regardless of the power model.

Figure 7 illustrates the relationship between the number of users and throughput (in Gbit/s) for different values of the renewable energy percentages (η) (0%, 25%, 50%, 75%, and 100%). The throughput increases proportionally with the number of users. In line with our expectations, it is clear from the figure that increasing the values of η will not affect the network throughput, compared to the scenario of $\eta = 0\%$, as shown in the zoomed-in view of the throughput values for 200 users.

4.2 Green users association illustration

Figure 8 illustrates the number of users assigned to each μBS for a scenario involving 400 users and various grid- and renewable energy-powered μBSs, considering renewable μBS percentages, ranging from 0% to 75% in 25% increments. Our optimization strategy demonstrates a clear preference for assigning more users to μBSs powered by renewable energy sources. The green columns illustrate the number of users allocated to μBSs powered by renewable energy. In contrast, the red columns present the number of users assigned to μBSs powered by the grid. This approach effectively minimizes power consumption from the grid. By leveraging a load-based strategy, our optimization aims to reduce the load on grid-powered microbase stations (μBSs). As a result, while it is necessary to activate some grid-powered μBSs, the power consumed by these active μBSs remains very low, akin to when the μBSs are off. Due to the remarkable efficiency demonstrated by the load-based strategy, it will be the focus for the remainder of this paper.

An example of users μBSs assignment with 50% renewable energy and for 400 users is illustrated in Fig. 9. In this figure, switched-on grid-powered μBSs are denoted by red diamonds, while green diamonds represent switch-off grid-powered μBSs. The yellow plus signs represent the renewable-powered μBS. The small blue plus signs represent users. Additionally, the black lines signify the connections between users and μBSs. We can observe that the optimization connects most of the users to the μBS powered by

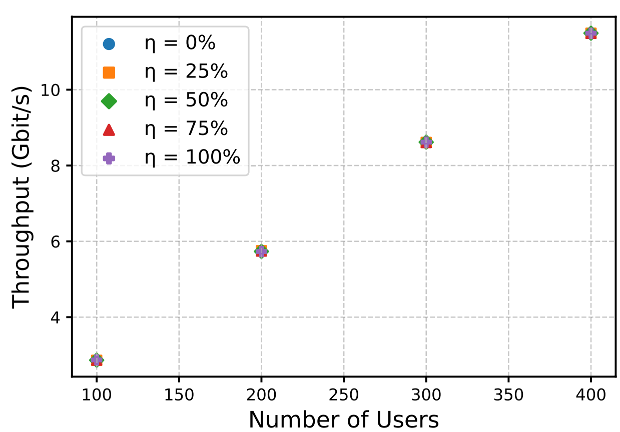

Fig. 7 Network throughput for different user numbers and renewable energy percentages. This figure shows the total network throughput in Gbit/s as the number of users increases from 100 to 400, under different renewable energy shares (0–100%). Throughput grows with user density and is not negatively impacted by renewable penetration, confirming that energy optimization does not harm network capacity

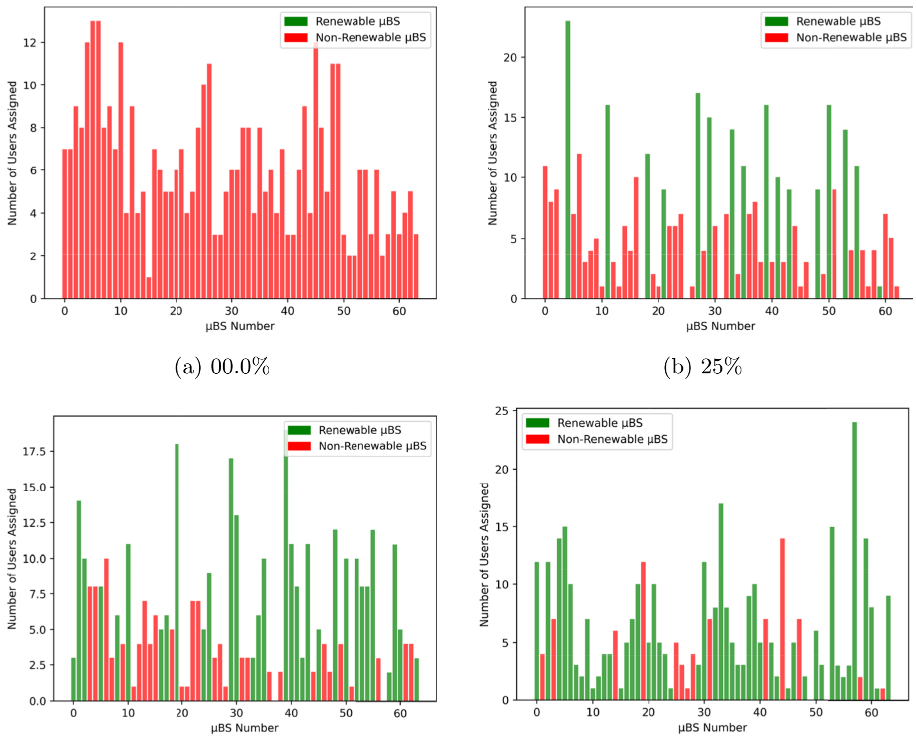

(a) 00.0%

(b) 25%

(c) 50%

(d) 75%

Fig. 8 User–µBS allocation versus renewable energy percentage. This multipanel figure **a**–**d** shows the number of users assigned to each µBS under renewable energy shares of 0%, 25%, 50%, and 75%. The optimization framework prioritizes renewable µBSs, significantly reducing the load on grid-powered µBSs

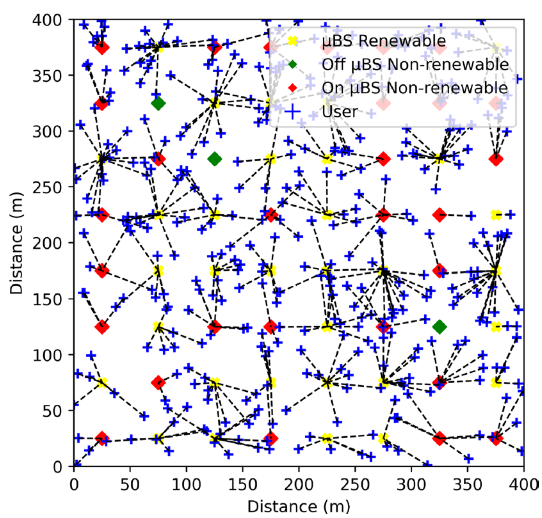

Fig. 9 User-µBS assignment with 50% renewable-powered µBSs. This figure shows a sample allocation of 400 users to 64 µBSs, half powered by renewable energy. Green diamonds represent switched-off grid-powered µBSs, red diamonds indicate active grid-powered µBSs, yellow crosses mark renewable-powered µBSs, and blue plus symbols denote users. Black lines represent active user-µBS connections, demonstrating prioritization of renewable resources

renewable energy sources, and when activating any grid-powered μBS, few users will be connected to it in order to reduce the grid-based power consumption.

4.3 Impact of interference modeling on SINR and throughput

To investigate the significance of inter-cell interference in our system, particularly in the context of mmWave communication, we evaluate how average SINR and throughput vary under different interference assumptions. In our model, first, each base station employs a single dipole antenna without beamforming, resulting in omnidirectional radiation and no inherent suppression of inter-cell interference.

However, to assess the implications of beamforming, we introduce a parametric interference scaling factor to emulate various degrees of directional isolation. Specifically, we simulate scenarios with inter-cell interference attenuated by 0 dB (no suppression), −10 dB, −20 dB, and −30 dB. These values mimic increasing levels of directionality and isolation that occur in practical mmWave systems using antenna arrays and beamforming.

The 0 dB case represents an interference-limited baseline with omnidirectional dipoles, whereas −20, −30 dB emulates practical beamforming isolation, approaching a noise-limited regime.

Taking into account the same configuration in Figs. 9 and 10 shows the average SINR under different interference scaling levels. The SINR improves dramatically as interference is suppressed, confirming that mmWave systems transition from interference-limited to noise-limited as directional gains increase. Figure 11 further illustrates the corresponding impact on throughput: The network evolves from a non-functional regime (39 Mbps at 0 dB) to a highly efficient regime (2600 Mbps at –30 dB). These

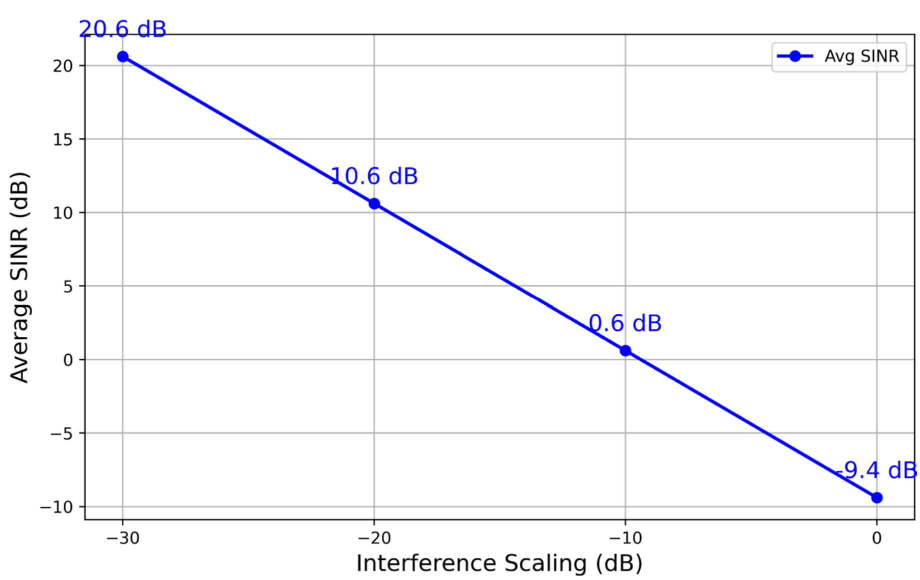

Fig. 10 Average SINR per user as a function of interference scaling. This figure illustrates the average SINR under different levels of inter-cell interference suppression (0 to −30 dB). As interference is reduced (simulating directional beamforming), SINR increases significantly, demonstrating the impact of interference on mmWave performance

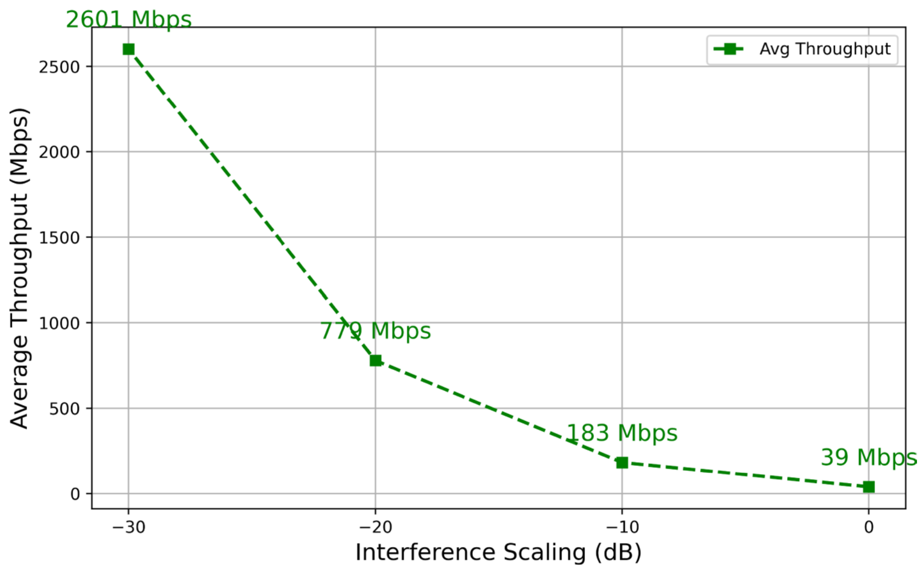

Fig. 11 Average throughput per user under different interference levels. This figure shows per-user throughput under different interference assumptions. Throughput increases from 39 Mbps at 0 dB suppression to 2600 Mbps at −30 dB, confirming that directional isolation greatly improves mmWave efficiency

results validate our inclusion of inter-cell interference in the analytical model, given our use of omnidirectional antennas.

4.4 Performance evaluation of the proposed solutions

Baseline: MAX-SINR User Association To benchmark the performance of our proposed heuristics, we introduce a classic MAX-SINR-based user-association strategy [26, 35]. In this method, each user is connected to the μBS (regardless of energy source) that provides the best SINR, subject to coverage and capacity constraints. This strategy prioritizes link quality without considering energy source or grid-power minimization. While it is computationally simple and widely used, it typically results in suboptimal energy consumption as it may over-utilize grid-powered μBSs.

Figure 12 shows the grid-power consumption of five algorithms—ILP, GUAS, RUAS, SUAS, and Max-SINR—under increasing levels of renewable energy integration: 25%, 50%, and 75% of BSs being powered by renewable energy sources. At 25% renewable energy, the ILP-based algorithm achieves the lowest grid-power usage at 273.524W, while Max-SINR and RUAS consume the most at 291.516W and 288.402W, respectively. As the renewable share increases to 50%, consumption drops across all methods, with ILP again leading at 176.689W and Max-SINR remaining highest at 202.548W.

At 75% renewable energy, all algorithms benefit from significant reductions, with ILP at 85.062W, followed by GUAS (89.214W), SUAS (92.328W), and both RUAS and Max-SINR at 96.48W. The performance gap narrows at higher renewable levels, indicating that increased renewable penetration mitigates differences in algorithm efficiency. Overall, the ILP consistently delivers the lowest grid power consumption, while RUAS and Max-SINR lag due to less optimized allocation strategies.

Figure 14 shows the power consumption patterns over 24 h for the proposed methods—ILP, GUAS, RUAS, and SUAS—when 50% of the μBSs are powered by

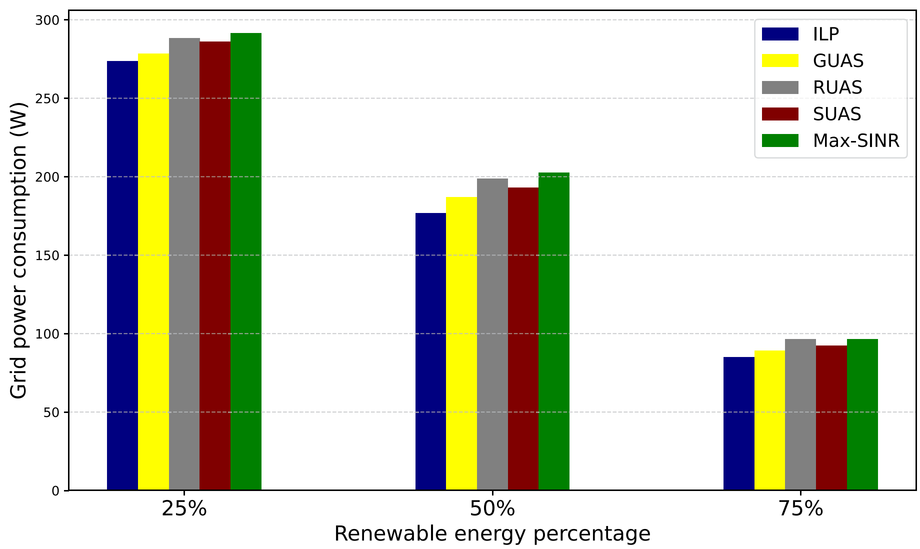

Fig. 12 Grid-power consumption for different solutions and renewable shares. This figure compares grid-power consumption across five user-association strategies (ILP, GUAS, RUAS, SUAS, and Max-SINR) at renewable shares of 25%, 50%, and 75%. The ILP consistently achieves the lowest consumption, while heuristic strategies approach ILP performance at higher renewable levels

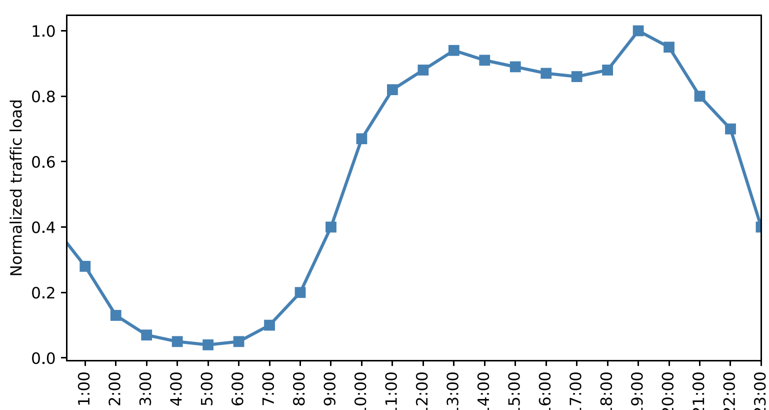

Fig. 13 Average traffic load profile over 24 h. This figure shows the normalized daily traffic variation used in the simulation model. Peak traffic occurs during daytime, while nighttime demand is lower, motivating μBS switching strategies

renewable energy. We take into account the daily traffic profile in Fig. 13, based on [36]. In this figure, the black horizontal line at 940.8 W denotes the "ALL μBSs on" condition, which serves as a reference point representing a scenario without renewable energy.

The inset within the main plot zooms in on the day hours, highlighting the fluctuations and enabling a closer look at comparative variations between the methods. Additionally, a bar chart inset on the right summarizes each method's average daily power consumption: ILP averages 159.15 Wh, GUAS 163.52 Wh, RUAS 183.50 Wh, and SUAS 175.73 Wh. Compared to the "ALL μBSs on" case, the power consumption

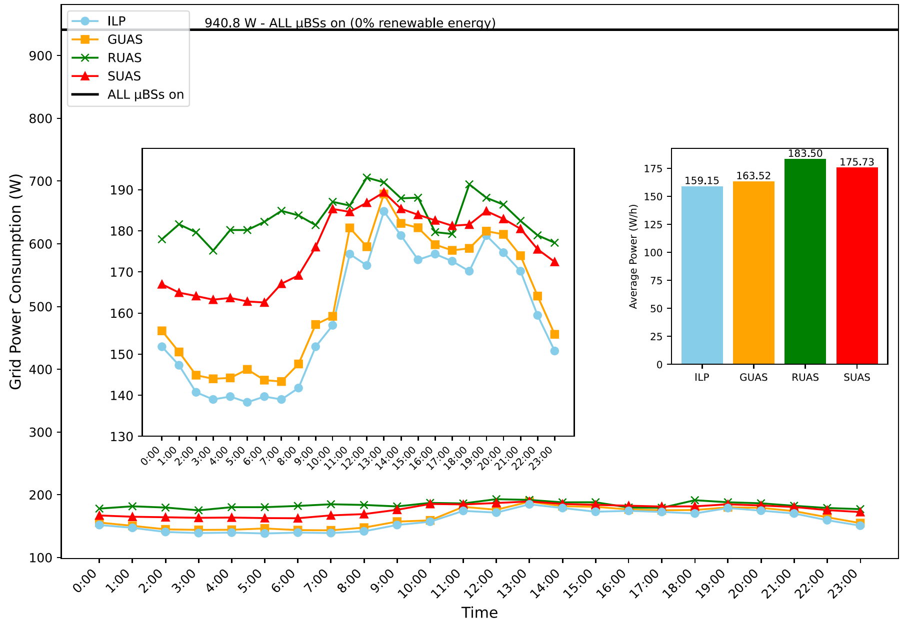

Fig. 14 Daily power consumption of proposed methods with 50% renewable μBSs. This figure presents hourly grid power consumption for ILP, GUAS, RUAS, and SUAS compared to the baseline, where all μBSs are always on. The inset bar chart shows average daily consumption, with ILP performing best, followed by GUAS, SUAS, and RUAS

Table 4 Runtime comparison of proposed and baseline algorithms (in seconds) assuming that 50% of the μBSs are powered by renewable source

Number of Users	ILP	GUAS	RUAS	SUAS	Max-SINR
100	2.420	0.860	0.421	0.547	0.302
200	7.636	2.100	1.025	1.854	0.860
300	21.981	2.956	1.645	2.223	1.290
400	57.80	4.025	2.015	2.875	1.881

reduction provided by ILP, GUAS, RUAS, and SUAS, respectively, is (83.1%, 82.6%, 80.4%, 81.3%).

In addition to analyzing the energy efficiency, we evaluate the computational efficiency of the proposed solutions. Table 4 presents the runtime in seconds for each algorithm under different user densities. The ILP solution incurs the highest computational cost, while the heuristic methods (GUAS, RUAS, SUAS) and the Max-SINR baseline execute significantly faster. The results confirm the practical efficiency of the proposed heuristics and validate their suitability for large-scale real-time applications in ultra-dense 6 G networks. Our simulations were conducted on a computer powered by an Intel(R) Core(TM) i5-1035G1 CPU operating at 1.00 GHz and supported by 8 GB GB RAM.

4.5 Europe level evaluation

In this subsection, we evaluate the impact of integrating renewable energy sources with dynamic load-based base station on–off switching on carbon emissions in Europe. According to [37], the total number of 5 G base stations deployed across Europe is 460,000. Average carbon dioxide emissions per kilowatt hour (kWh) of electricity in Europe's six largest economies—Germany, France, the United Kingdom, Italy, Spain, and the Netherlands—were 253 (gCO_2) through November 2023 based on [38]. Based on the heat map provided in [39], the tax cost of generating 1 ton of CO_2 in Europe is 50 (€/tCO_2e). Assuming that each base station consumes 3000 W of power per day, as stated in [19]. The total energy consumption per year for the 460,000 BSs is 5×10^6 kWh. This results in total CO_2 emissions of 1.27×10^5 tons annually. The corresponding carbon tax cost amounts to approximately €6.35 million per year.

Figure 15 shows the impact of integrating renewable energy into base station operations on carbon tax savings and CO_2 emissions reductions. The x-axis represents the renewable energy percentage (0%, 25%, 50%, 75%), while the left y-axis indicates the carbon tax savings in million euros, and the right y-axis shows the corresponding CO_2 emissions reductions in tons. The dashed lines represent the baseline values without any renewable energy integration. The bars illustrate how increasing renewable energy reduces both the carbon tax cost and CO_2 emissions, highlighting the environmental and financial benefits of renewable energy adoption. By utilizing the ILP solution, for example, with a dynamic load-based linear power model and assuming 50% of the BSs are powered by renewable energy, the CO_2 emissions would be reduced to 21,463 tons. This reduction leads to savings of about €5.28 million in annual carbon tax costs.

5 Conclusion

In this paper, we propose optimization solutions to address the problem of user association with green power maximization in networks beyond 5 G ultra-dense. We consider the dynamic load-based μBS switching strategy with the integration of renewable energy sources, aiming at reducing the grid-power μBSs power consumption and maximizing the dependability of the network on renewable energy sources. We formulated the problem as an ILP framework under various connectivity, power, and QoS

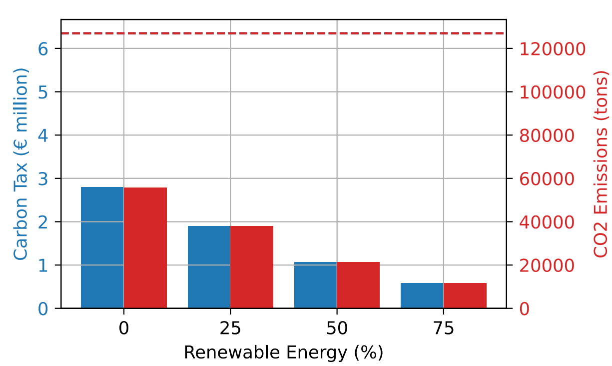

Fig. 15 CO_2 emissions and carbon tax savings with renewable integration. This figure shows the reduction in annual CO_2 emissions and carbon tax savings at renewable energy shares of 0%, 25%, 50%, and 75%. Integration of renewables significantly reduces emissions and costs, with 50% renewables saving approximately €5.28 million annually

constraints. Given the NP-hardness of the problem, we have proposed three heuristic solutions, namely GUAS, RUAS, and SUAS. We conducted extensive simulations to evaluate the performance of our proposed approaches, considering different numbers of users and different renewable energy percentages. The simulation results showed the ability of our proposed approaches to reduce grid-based power consumption by more than 80%. Moreover, we have shown the applicability of our proposed optimization in reducing the CO_2 up to 83%, considering the scenario that 50% of the μBSs are powered by renewable energy sources.

Our current model assumes that renewable μBSs are supported by sufficient energy storage to maintain operation when harvesting is not possible (e.g., at night). While this simplifies the problem to focus on spatial user association and switching, it omits the temporal dynamics of energy harvesting and storage. In future work, we plan to integrate battery charge/discharge dynamics and time-varying renewable profiles (e.g., solar irradiance patterns) to capture intermittency and storage constraints more accurately. Furthermore, we plan to integrate per-user multiconnectivity (dual, triple, quadruple) connectivity and evaluate robustness-energy trade-offs. Moreover, while this study assumes single-antenna dipoles for tractability, future extensions will incorporate multiple-antenna systems, such as massive MIMO and near-field XL-MIMO [40, 41].

Abbreviations

6 G	Sixth generation (mobile network)
BS	Base station
μBS	Microbase station
mmWave	Millimeter wave
SINR	Signal-to-interference-plus-noise ratio
ILP	Integer linear programming
NP-hard	Non-deterministic polynomial-time hard
SCP	Set cover problem
GUAS	Greedy green user allocation strategy
RUAS	Random user allocation strategy
SUAS	Sequential user allocation strategy
QoS	Quality of service
CO_2	Carbon dioxide
Opex	Operational expenditure
FR2	Frequency range 2 (5 G/6 G band, 24–52 GHz)
MIMO	Multiple input multiple output
ICT	Information and Communication Technology
GSMA	Global System for Mobile Communications Association
ITU	International Telecommunication Union
IMT-2030	International Mobile Telecommunications 2030 Framework

Acknowledgements
This work, EKÖP-24-4-I, was supported by the University Researcher Scholarship Program (Egyetemi Kutatói Ösztöndíj Program) funded by the Ministry of Culture and Innovation (Kulturális és Innovációs Minisztérium)by the National Research, Development, and Innovation Fund (Nemzeti Kutatási, Fejlesztési és Innovációs Alap) under the EKÖP-24-4-I-BME-7 funding scheme. This work was also supported by the CHIST-ERA grant SAMBAS (CHIST-ERA-20-SICT-003) funded by FWO, ANR, NKFIH, and UKRI. Additionally, the work was also supported by BME HUN-REN Cloud Applications through project 2019–2.1.11-TET-2020-00183 under the 2019–2.1.11-TET funding scheme.

Author Contributions
AF was involved in conceptualization, methodology, software, and writing—original draft; TC took part in supervision, methodology, and writing—review and editing; IG was responsible for validation and writing—review and editing; JF participated in writing—review and editing and resources. All authors read and approved the final manuscript.

Funding
Open access funding provided by Budapest University of Technology and Economics. This work was supported by the University Researcher Scholarship Program (EKÖP-24-4-I) funded by the Ministry of Culture and Innovation by the National Research, Development, and Innovation Fund under the EKÖP-24-4-I-BME-7 funding scheme. It was also supported by the CHIST-ERA grant SAMBAS (CHIST-ERA-20-SICT-003) funded by FWO, ANR, NKFIH, and UKRI, as well as by

BME HUN-REN Cloud Applications through project 2019–2.1.11-TET-2020-00183 under the 2019–2.1.11-TET funding scheme.

Data Availability
Data sharing is not applicable to this article as no datasets were generated or analyzed during the current study.

Code Availability
The simulation code developed for this study is not publicly available due to institutional policy but can be reproduced based on the methodology described in the manuscript.

Declarations

Conflict of interest
The authors declare that they have no competing financial or non-financial interests.

Ethics approval and consent to participate
Not applicable.

Consent for publication
Not applicable.

Received: 18 September 2025 Accepted: 19 February 2026
Published online: 05 March 2026

References
1. ITU-R: Framework and overall objectives of the future development of IMT for 2030 and beyond. Draft new recommendation. M.[IMT.FRAMEWORK FOR 2030 AND BEYOND] (2023)
2. B. Romanous, N. Bitar, A. Imran, H. Refai, *Network densification: Challenges and opportunities in enabling 5G*, in *2015 IEEE 20th International Workshop on Computer Aided Modelling and Design of Communication Links and Networks (CAMAD)* (2015), pp. 129–134. https://doi.org/10.1109/CAMAD.2015.7390494
3. A. Fayad, T. Cinkler, Optimal Slicing of mmWave Micro Base Stations for 5G and Beyond. J. Netw. Netw. Appl. **3**(3), 99–108 (2023)
4. W. Hong, Z.H. Jiang, C. Yu, D. Hou, H. Wang, C. Guo, Y. Hu, L. Kuai, Y. Yu, Z. Jiang et al., The role of millimeter-wave technologies in 5G/6G wireless communications. IEEE J. Microw. **1**(1), 101–122 (2021)
5. Ericsson: Improving Energy Performance in 5G Networks and Beyond. Ericsson Technology Review (2022). Accessed: 2024 Nov, 11
6. B. Labs, Energy Efficiency in Next-Generation Mobile Networks. Technical report, Nokia Bell Labs (2022). Accessed: 2024–11-11. https://www.bell-labs.com/institute/white-papers/energy-efficiency-in-next-generation-mobile-networks/gref
7. ATIS: Next G Alliance Green G: The Path Toward Sustainable 6G. White paper (2022). https://nextgalliance.org/white_papers/green-g-the-path-towards-sustainable-6g/
8. GSMA: The Enablement Effect: The impact of mobile communications technologies on carbon emission reductions. Report (2019)
9. M. Soleymani, D., E. Roth-Mandutz, in *6G Energy Efficiency and Sustainability White Paper 6G Energy Efficiency and Sustainability* (2023)
10. M.J.B. Kabeyi, O.A. Olanrewaju, Sustainable energy transition for renewable and low carbon grid electricity generation and supply. Front. Energy Res. **9**, 1032 (2022)
11. C. Andersson, J. Bengtsson, G. Byström, P. Frenger, Y. Jading, M. Nordenström, Improving energy performance in 5G networks and beyond. Ericsson Technol. Rev. **2022**(8), 2–11 (2022). https://doi.org/10.23919/ETR.2022.9911220
12. W. Wu, C.-S. Yang, I.-K. Fu, P.-K. Liao, D. Calin, M. Fan, Revisiting the system energy footprint and power efficiency on the way to sustainable 6G systems. IEEE Wirel. Commun. **29**(6), 6–8 (2022)
13. S. Maiti, S. Juneja, Energy efficiency techniques in 5g/6g networks: green communication solutions, in *Advances in Data-Driven Computing and Intelligent Systems*. ed. by S. Das, S. Saha, C.A. Coello, J.C. Bansal (Springer, Singapore, 2024), pp.407–423
14. Q. Wu, G.Y. Li, W. Chen, D.W.K. Ng, R. Schober, An overview of sustainable green 5G networks. IEEE Wirel. Commun. **24**(4), 72–80 (2017)
15. T. Wu et al., Fluid antenna systems enabling 6g: Principles, applications, and research directions. arXiv:2412.03839 (2024)
16. T. Wu, C. Pan, K. Zhi, H. Ren, M. Elkashlan, C.-X. Wang, R. Schober, X.-H. You, Exploit high-dimensional ris information to localization: What is the impact of faulty element? IEEE J. Sel. Areas Commun. **42**(10), 2803–2819 (2024)
17. L. Mai, H. Luo, Q. Zhang, Integrated over-the-air computation and non-orthogonal multiple access communication in wireless uplink systems. IEEE Trans. Wirel. Commun. **23**(9), 11433–11443 (2024)
18. M. Rubina Aktar, M. Shamim Anower, Z.I. Sarkar, M., Sayem, A.S.M., Rashedul Islam, M., Akash, A.I., Rumana Akter Rume, M., Moloudian, G., Lalbakhsh, A., Energy-efficient hybrid powered cloud radio access network (C-RAN) for 5G. IEEE Access **11**, 3208–3220 (2023). https://doi.org/10.1109/ACCESS.2023.3234190

19. C.-S. Yang, C. Lin, I.-K. Fu, *Carbon-neutralized joint user association and base station switching for green cellular networks*, in *2023 IEEE International Conference on Communications Workshops (ICC Workshops)* (2023), pp. 1594–1599. https://doi.org/10.1109/ICCWorkshops57953.2023.10283575
20. A. El Amine, H.A.H. Hassan, L. Nuaymi, Battery-aware green cellular networks fed by smart grid and renewable energy. IEEE Trans. Netw. Serv. Manag. **18**(2), 2181–2192 (2021). https://doi.org/10.1109/TNSM.2020.3038302
21. H. Al Haj Hassan, K. Deep Singh, L. Nuaymi, *Grid energy consumption of mixed-traffic cellular networks with renewable energy sources*, in *2016 IEEE Online Conference on Green Communications (OnlineGreenComm)* (2016), pp. 1–6. https://doi.org/10.1109/OnlineGreenCom.2016.7805398
22. J. Han, N. Liu, Y. Huang, Z. Zhou, Collaborative optimization of distribution network and 5G mobile network with renewable energy sources in smart grid. Int. J. Electr. Power Energy Syst. **130**, 107027 (2021). https://doi.org/10.1016/j.ijepes.2021.107027
23. J. Gong, J.S. Thompson, S. Zhou, Z. Niu, Base station sleeping and resource allocation in renewable energy powered cellular networks. IEEE Trans. Commun. **62**(11), 3801–3813 (2014). https://doi.org/10.1109/TCOMM.2014.2359883
24. L. Pang, H. Zhao, Y. Zhang, Y. Chen, Z. Lu, A. Wang, J. Li, Energy-efficient resource optimization for hybrid energy harvesting massive MIMO systems. IEEE Syst. J. **16**(1), 1616–1626 (2022). https://doi.org/10.1109/JSYST.2021.3074542
25. H. Wang, M. Huang, Z. Zhao, Z. Guo, Z. Wang, M. Li, Base station wake-up strategy in cellular networks with hybrid energy supplies for 6G networks in an IoT environment. IEEE Internet Things J. **8**(7), 5230–5239 (2021). https://doi.org/10.1109/JIOT.2020.3045270
26. A. Fayad, T. Cinkler, Energy-efficient joint user and power allocation in 5g millimeter wave networks: a genetic algorithm-based approach. IEEE Access **12**, 20019–20030 (2024)
27. A. Fayad, T. Cinkler, J. Rak, 5G millimeter wave network optimization: dual connectivity and power allocation strategy. IEEE Access **11**, 82079–82094 (2023). https://doi.org/10.1109/ACCESS.2023.3300960
28. A. Fayad, T. Cinkler, *Power consumption optimization in 5G/6G mmWave networks with user multi-connectivity*, in: *2024 IEEE Pacific Rim Conference on Communications, Computers and Signal Processing (PACRIM)* (2024), pp. 1–6. https://doi.org/10.1109/PACRIM61180.2024.10690210
29. GSMA: Renewable Energy for Mobile Towers: Opportunities and Challenges in the Transition to Net Zero (2021). https://www.gsma.com/solutions-and-impact/connectivity-for-good/mobile-for-development/gsma_resources/renewable-energy-for-mobile-towers-opportunities-for-low-and-middle-income-countries/
30. C. Andersson, J. Bengtsson, G. Byström, P. Frenger, Y. Jading, M. Nordenström, Improving energy performance in 5G networks and beyond. Ericsson Technol. Rev. (2022)
31. T.S. Rappaport, G.R. MacCartney, M.K. Samimi, S. Sun, Wideband millimeter-wave propagation measurements and channel models for future wireless communication system design. IEEE Trans. Commun. **63**(9), 3029–3056 (2015). https://doi.org/10.1109/TCOMM.2015.2434384
32. R.M. Karp, On the computational complexity of combinatorial problems. Networks **5**(1), 45–68 (1975)
33. A.M. Hamed, R.K. Rao, *Evaluation of capacity and power efficiency in millimeter-wave bands*, in: *2016 International Symposium on Performance Evaluation of Computer and Telecommunication Systems (SPECTS)* (IEEE, 2016), pp. 1–6
34. Á. Ladányi, T. Cinkler, Resilience-throughput-power trade-off in future 5G photonic networks. Photon Netw. Commun. **37**, 296–310 (2019)
35. J.G. Andrews, Seven ways that hetnets are a cellular paradigm shift. IEEE Commun. Mag. **51**(3), 136–144 (2013)
36. P. Frenger, Y. Jading, J. Bengtsson, 5G energy consumption: the impact of 5G NR. Ericsson Blog (2021). https://www.ericsson.com/en/blog/2021/10/5g-energy-consumption-impact-5g-nr
37. 5G Observatory: 5G Observatory Report-June 2024. Technical report (2024). Accessed: 2023–11-15. https://5gobservatory.eu/wp-content/uploads/2024/07/BR-20_5G-Observatory-Report-June-2024.pdf
38. Reuters: Europe's top economies slash carbon intensity of electricity. Accessed: 2023–11-15 (2023)
39. S. Oğuz, Visualized: The Price of Carbon Around the World in 2024. Accessed: 2023–11-15 (2024)
40. K. Zhi, C. Pan, H. Ren, K. Wang, M. Elkashlan, M. Di Renzo, R. Schober, H.V. Poor, J. Wang, L. Hanzo, Two-timescale design for reconfigurable intelligent surface-aided massive mimo systems with imperfect csi. IEEE Trans. Inf. Theory **69**(5), 3001–3033 (2022)
41. K. Zhi, C. Pan, H. Ren, K.K. Chai, C.-X. Wang, R. Schober, X. You, Performance analysis and low-complexity design for xl-mimo with near-field spatial non-stationarities. IEEE J. Sel. Areas Commun. **42**(6), 1656–1672 (2024)

Publisher's Note